Regular Article

Deep Learning Based Cooperative MIMO Systems for Wireless Body Area Networks

Thi Thanh Tam Bui[1], Xuan Nam Tran[2], Anh Huy Phan[1]

[1] Academy of Military Science and Technology, Hanoi, Vietnam
[2] Le Quy Don Technical University, Hanoi, Vietnam

Correspondence: Xuan Nam Tran, namtx@mta.edu.vn
Communication: received 16 January 2024, revised 27 January 2024, accepted 30 January 2024
Online publication: 30 January 2024, Digital Object Identifier: 10.21553/rev-jec.352
The associate editor coordinating the review of this article and recommending it for publication was Prof. Hoang Van Phuc.

Abstract– **Wireless Body Area Network (WBAN) is widely applied in various fields, including healthcare, sports, wellness, and assistive technologies, by offering the benefits of convenience, reliability, low latency, privacy, and customization. However, the propagation characteristics of the WBAN channel can impact the reliability of transmission, which is particularly crucial in healthcare systems. To address this issue, this article presents a novel approach using deep learning-based cooperative Multiple-Input Multiple-Output (MIMO) systems that leverage the autoencoder (AE) technique. In our proposed approach, we utilize the AE-based cooperative MIMO systems with two different techniques: Amplify-and-Forward (AE-AF) and Decode-and-Forward (AE-DF). The AE-AF scheme operates without needing training parameters at the relay node, whereas the AE-DF scheme necessitates training parameters at the relay node. Both schemes aim to overcome challenges such as multipath propagation phenomena, thereby enhancing the performance of on-body communication systems. Additionally, we introduce two combinators, Minimum Mean Square Error (MMSE) scheme and Radio Transformation Network (RTN), to effectively mitigate co-channel interference (CCI) in the received signal streams and improve the bit error rate (BER) performance of the AE-AF and AE-DF systems. We assess the performance of these systems in scenarios with and without direct links. Simulation results demonstrate significant performance improvements compared to baseline cooperative MIMO systems using MMSE combining, namely AF-MMSE and DF-MMSE systems. Notably, the proposed systems employing RTN combination, including both direct and relay paths, achieve a 7.5 dB gain over the baseline when all nodes are equipped with two transceiver antennas.**

Keywords– **WBAN, cooperative MIMO, deep learning, autoencoder.**

1 Introduction

Wireless Body Area Networks (WBANs) are recognized as networks designed to gather and transmit human body-related data, such as heart rate, blood pressure, electroencephalogram (EEG), and electrocardiogram (ECG), to healthcare centres or doctors for monitoring purposes and delivering timely health alerts to users. These networks are rapidly developing in various fields of life, particularly in medicine and healthcare [1]. The signal transmission process in WBAN complies with the IEEE 802.15.6 standard, which includes various frequency bands, including narrowband bands such as the Human Body Communication (HBC), Medical Implant Communication System (MICS), Industrial, Scientific and Medical (ISM), and wideband Ultra-Wide Band (UWB) band. Additionally, WBAN incorporates five main channel models classified based on the communication links between nodes placed inside, on, and near the body (CM1-CM5) [2, 3]. In healthcare and wellness applications, WBAN demonstrates several advantages, including continuous monitoring of vital signs, timely health status alerts, and allowing individuals to maintain their normal activities.

However, WBAN also faces communication challenges such as transmission loss, multipath channels, and shadowing phenomena [3]. Additionally, WBAN applications impose network quality requirements such as reliable transmission, prolonged energy-saving for network longevity, and user information security, etc. [1, 4]. When assessing the performance of WBAN systems, reliability emerges as one of the most critical communication metrics, especially in healthcare applications. Therefore, to overcome the challenges and meet the network's performance requirements, numerous studies proposed various communication solutions, such as error correction codes, interference suppression codes to improve reliability [5, 6], energy-efficient routing solutions to prolong network lifetime [7], information security [8], cooperative communication [9], multiple-antenna transmission [10]. Significantly, the explosive growth of artificial intelligence, deep learning, and machine learning techniques applied in communication systems has helped optimize the parameters of functional blocks or the entire system through the training process, enhancing the system's performance [11].

In addition, along with the development of technologies such as Microelectromechanical systems (MEMS), research on applying antennas in the 60 GHz frequency range [12], and the development of new wearable sensors with lightweight, low power consumption, flexi-

bility, and compactness using suitable materials [13], they significantly contribute to the substantial advancement of WBAN in various areas of life through the implementation of new communication techniques that enhance reliability while remaining compact and user-friendly.

The nodes transmit information according to the star, two-hop relay or mixed topologies based on the IEEE 802.15.6 standard. Due to body-worn nodes moving based on user activities, sensor nodes can experience obstruction by body parts, which can either block the direct transmission path to the central node or cause significant signal attenuation in the transmission path to the central node due to transmission distance or tissue absorption. This obstruction reduces the reliability performance or leads to an escalation in the energy consumption of the sensor nodes [4]. Cooperative transmission solutions allow information to be transmitted to the destination node through one or multiple relay nodes. The destination node combines signals from both the direct and relayed paths, thereby overcoming obstruction issues and improving the reliability of information transmission in the WBAN [9, 14]. Aiming to exploit the spatial diversity of distributed sensor nodes, studies [14–16] proposed the utilization of cooperative Single-Input Single-Output (SISO) communications within WBANs to enhance the performance of error rates and energy efficiency. Y. Zhang et al. introduced a schedule for automatic dynamic switching between direct and relay-assisted transmission of single antenna systems based on channel conditions to improve transmission reliability and save energy in relay nodes in WBAN [9].

Multiple Input Multiple Output (MIMO) systems are employed to enhance the reliability of WBANs because this technique enables increased system capacity and achieves spatial multiplexing gains. The works [17, 18] show that using MIMO can help to reduce the impact of shadowing and multipath fading to improve transmission reliability. The study [19] proposes using a 2×2 MIMO Spatial Division Multiplexing (SDM) technique for on-body narrowband systems operating at a frequency of 2.45 GHz using Planar Inverted-F Antennas (PIFAs). The study examines spatial correlation matrices and demonstrates that the on-body antenna movement generates significant decorrelation among subchannels, even when LOS connections are present. Additionally, the findings indicate that the capacity achieved by the MIMO system is twice that of the SISO system. The studies [20, 21] introduces MIMO antennas designed for the frequency range of 2.4 GHz - 30 GHz and Terahertz, intended for WBAN applications. The research results indicate that the proposed antenna is a good solution for WBAN applications. Additionally, a work [22] proposes the use of a cooperative sensor scheme employing network coding to create a virtual MIMO system for monitoring sleep apnea. This solution allows for energy efficiency and reduces the impact of phase dispersion. A work [23] proposes an MIMO system operating in the 5.8 GHz ISM frequency band to mitigate fading.

A work [10] proposes a cooperative MIMO transmission system (with and without a direct path) between implantable and wearable sensors equipped with a single antenna and a receiver device placed near the body with two antennas. The solution uses an index modulation technique to counteract inter-channel interference (ICI) and save energy consumption for the network. A cooperative massive MIMO-SDM system is proposed for body-centric communication to increase the channel capacity in [24]. Another approach to improving the system throughput and transmission reliability of WBANs network coding is combined with MIMO cooperative communication in [25]. In the study [8], researchers put forward a dynamic configuration and virtual cooperative MIMO approach grounded in game theory. The objective is to ensure the security of transmitted information while achieving energy savings. Based on simulation results, it is evident that the virtual cooperative MIMO configuration method proposed, which is grounded in game theory, can enhance the security capabilities of individual devices and extend the lifespan of the network when compared to non-cooperative approaches. Moreover, a study [26] proposes the use of a cooperative MIMO system for the body channel. Research results indicate that the proposed scheme reduces energy consumption and enables long-distance transmission compared to a cooperative SISO system. Other studies [27–29] concentrate on signal combination techniques applied to cooperative MIMO-SDM systems employing Amplify-and-Forward (AF) and Decode-and-Forward (DF) methods.

In recent years, deep learning (DL) techniques have garnered significant research interest and found application in communication systems at large, including WBANs, to enhance overall system performance [4, 30–35]. The reinforcement learning (RL) algorithm is introduced to enhance secure transmission with minimal eavesdropping rates [34] and to ensure reliable transmission of emergency data from sensors to the central unit [35] in WBANs. A study [33] introduces the Frame Aggregation Organization method based on Deep Q-learning Network, abbreviated as DQN-FATOA, significantly reduced latency and energy consumption, improving the data transmission capability of WBANs compared to traditional scheduling methods. The DeepBAN system utilizes a deep learning approach, specifically the Time Convolutional Network (TCN), for channel prediction, as demonstrated in work cited as [31].The results show that DeepBAN improves the system's energy efficiency by up to 15% compared to random scheduling. In addition, a channel prediction model for MIMO transmission in WBAN using DL is proposed in the research [30] for underground mining environments.

The solution of applying deep learning techniques based on the autoencoder (AE) for communication systems is a research direction that has attracted the interest of many research groups [11, 32, 36]. In this approach, the entire system, including the transmitter, receiver and channel, is represented by neural networks

similar to an AE architecture. Furthermore, this solution improves system reliability through the automatic synchronization learning capability of the system's trainable parameters, achieved through the training process to minimize transmitted symbol errors and estimation errors at the receiver.

Several studies have proposed the use of AE for point-to-point single-antenna communication systems [11, 32, 37], abbreviated as AE-SISO, or with the support of relay nodes [36, 38]. A new optimized architecture for the HBC system to achieve high data transmission speed is designed and deployed through the autoencoder technique in work [32]. By adopting an AE-based approach, the HBC system design surpasses the traditional method, significantly improving up to 2 dB in the block error rate. On the one hand, the AE-SISO system's performance surpasses the traditional SISO system with Hamming encoding and the maximum likelihood (MLD) estimator with a single training phase thanks to the simultaneous modulation and encoding solution in work [11]. On the other hand, in work [37], the AE-SISO system tackles the challenges of imperfect channel information estimation by implementing two consecutive training phases. This approach aims to enhance the AE-SISO system's performance while dealing with the transmission channel's effects and outperforms the conventional QPSK modulation system.

In the study [36], Yuxi Lu et al. proposes a cooperative DF based AE-SISO system, in which the source, destination and relay nodes are represented by neural networks.The channel estimation and equalization are performed by both the relay and destination nodes using a Radio Transformation Network (RTN) network simultaneously, liked in [11]. The system is trained in two sequential phases at a fixed Signal to Noise (SNR) value or a range of SNR values over the fading channel. When modulation and encoding techniques are combined, the performance of the proposed AE system, which lacks channel state information (CSI), closely matches that of a conventional cooperative SISO system utilizing DF with a 1-bit pilot. Likewise, a study [38] demonstrates that utilizing the AE technique in an AF relay system yields better results than the traditional system employing Hamming encoding and an MLD estimator. When utilizing gray code formatting for the symbols, the bit-wise AE scheme outperforms the symbol-wise AE scheme.

The studies [39–42] proposed employing the AE technique for MIMO systems to enhance the error rate performance. In their study [39], T. Erpek et al. presented a closed-loop SWAE-MIMO $N_t \times N_r$ system featuring N_t transmitting antennas and N_r receiving antennas. When employing two transceiver antennas, the simulation results reveal that the AE-MIMO system with constant CSI exhibits a significant performance advantage of over 10 dB compared to the conventional MIMO system that utilizes an MMSE estimator at a symbol error rate (SER) of 10^{-2}. Similarly, the works [40, 41] propose the structure of symbol-wise AE-MIMO systems over fading channels, the AE-MIMO 2×1 using Space-Time Block Code (STBC) and SDM AE-MIMO 2×2 schemes. In the study [40], where full CSI knowledge was assumed, the AE-MIMO system outperformed the conventional MIMO system employing the Singular Value Decomposition (SVD) technique in terms of performance.

The proposed STBC systems also outperform the conventional STBC systems in [40, 41]. Additionally, the study [42] proposes open-loop AE-MIMO-SDM schemes using symbol and bit-wise labeling methods with different detectors. The simulation results clearly indicate that the proposed schemes exhibit significantly superior performance compared to conventional MIMO systems that utilize MMSE estimation. Remarkably, when equipped with two transceiver antennas, the AE-MIMO-RTN system demonstrates comparable BER performance to the conventional MIMO system utilizing Maximum Likelihood Detection.

In previous studies, communication within WBANs primarily utilizes cooperative single-antenna, MIMO and virtual MIMO systems to reduce fading effects and enhance communication performance. The research on cooperative MIMO with space division multiplexing in WBANs is still limited, and there have been no studies on cooperative MIMO with space division multiplexing using DL techniques for communication between nodes over the on-body channel. Based on the MIMO systems using AE as proposed in [42], we propose AE-based cooperative MIMO systems for two-hop communication links within WBAN. In traditional MIMO cooperative systems, the parameters of the source node, destination node, and relay node are pre-computed, while in AE-based MIMO cooperative systems, these parameters can be automatically learned partially or entirely during training to optimize the performance of the bit error rate. Compared to previous research, we can summarize our main contributions as follows:

- We propose two AE-based cooperative MIMO systems (AE-AF) for on-body communication to achieve optimal performance. These systems utilize MMSE and RTN combinators at the destination nodes, denoted as AE-AF-MMSE and AE-AF-RTN. They undergo a single-phase training process to jointly optimize parameters from the source node, relay node, and destination node.
- We also introduce two DF-based cooperative MIMO systems using the AE technique with MMSE and RTN combining schemes, abbreviated as AE-DF-MMSE and AE-DF-RTN. The AE-DF systems exhibit superior error performance compared to AE-AF, thanks to their ability to avoid noise amplification at the relay node. Furthermore, two sets of parameters, θ_{RxR} and θ_{TxR}, at the relay node are trained synchronously with the entire system.
- Simultaneously, we present the training algorithms for AE-based cooperative systems, which combine signals from a direct transmission and a relay transmission to improve BER performance.
- Finally, simulation results demonstrate that the proposed systems outperform the AF-based cooperative MIMO using MMSE combinator

in work [27], abbreviated as AF-MMSE, DF-based cooperative MIMO using MMSE and ZF combinator [29], abbreviated as DF-MMSE, DF-ZF, respectively. The BER of AF-MMSE, DF-MMSE and DF-ZF are called baselines.

Paper outline: The conventional cooperative MIMO-SDM system model is presented in Section 2. We introduce the proposed AE-based cooperative MIMO WBAN system using AF and DF techniques in Section 3. Section 4 analyzes the simulation results, and finally, we summarize the conclusions in Section 5.

Notations: Lower and upper case bold letters,**a** and **A**, denote vectors and matrices, respectively; $\mathbf{A} \in \mathbb{C}^{N\times N}$, $\mathbf{A} \in \mathbb{R}^{N\times N}$ refer to matrix **A** belongs to the set of complex and real matrices with a size of N rows and N columns, respectively; $\|\mathbf{a}\|^2$ denotes the Euclidean norm-2 of a vector **a**, $(\cdot)^H$,$(\cdot)^T$, $(\cdot)^{-1}$ denote the conjugate transpose, the transpose inverse of the matrix, respectively.

2 System Model

A WBAN typically has a 3-tier structure, each with its functions and characteristics [1]. The first tier, the intra-WBAN, comprises sensors positioned inside, on, and around the body, along with a personal device. Sensors can be interconnected to transmit information to the personal device acted as a gateway connecting the intra-WBAN to the second tier of the network. Transmission reliability is a critical criterion for ensuring the effectiveness of WBAN, particularly in healthcare applications [43]. However, due to users' activities and positions, some nodes may become obstructed by body parts, leading to occasional failures in the direct transmission of signals from sensors to personal devices (single-hop link) [44, 45]. Therefore, a cooperative MIMO communication system is proposed for intra-WBAN, abbreviated as WBAN, as presented in Figure 1. This scheme, supported by the IEEE 802.15.6 standard, aims to alleviate the impacts of multipath channels, enhance capacity, and improve error rate performance.

The on-body communication system comprises sensors transmit data, called source nodes (S_1, S_2), sensors perform the signal forwarding function, called relay nodes (R_1, R_2, R_3) and a personal device/destination node (PD/D) receives signals from the sensors within the WBAN. The source nodes can transmit to the destination node through either a single-hop model ($S_1 \rightarrow D$, $S_2 \rightarrow D$) or a two-hop cooperative model. The sensor S_2, worn on the right wrist, should be able to transmit cooperatively to the destination node, worn on the left waist, through both a direct and a relay path, represented by blue arrows, or relay paths in case user movements obstruct the direct transmission, represented by red arrows.

Figure 2 illustrates a detailed diagram of the cooperative MIMO transmission protocol from the source node to the destination node using both a direct path and relay paths. The source, destination, and relay nodes are outfitted with N antennas to facilitate receiving and transmitting. According to this model, the channel matrices between the source and destination, between the source and relay node, and between the relay node and destination are $\mathbf{H}^c_{sd} \in \mathbb{C}^{N\times N}$, $\mathbf{H}^c_{sr} \in \mathbb{C}^{N\times N}$ and $\mathbf{H}^c_{rd} \in \mathbb{C}^{N\times N}$, respectively. In this context, the indices s, r, and d refer to the source node, the relay node, and the destination node, respectively; the index c signifies complex-valued matrices and vectors.

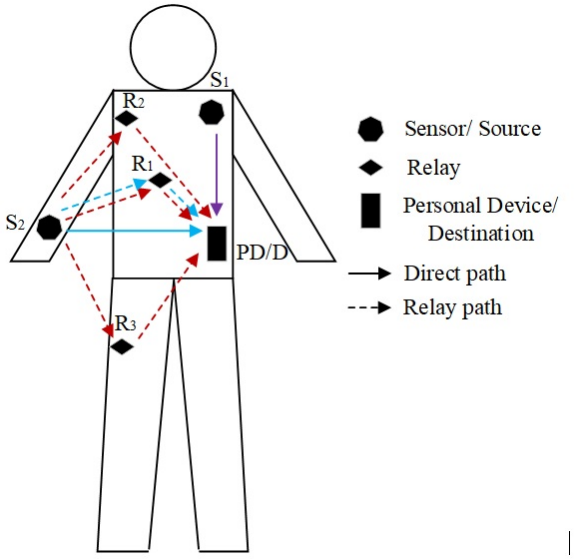

Figure 1. A intra-WBAN system.

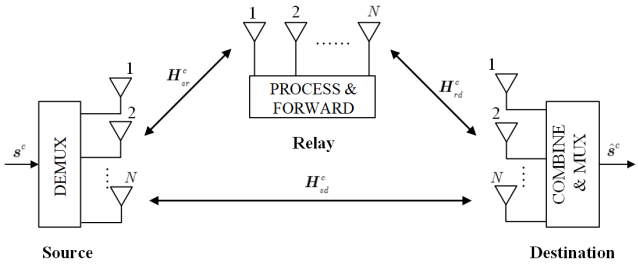

Figure 2. A cooperative MIMO communication system.

The communication protocol in the cooperative network is implemented on two time slots [29]. In the first time slot, the source node simultaneously transmits signals $\mathbf{s}^c$ to the relay and destination nodes. The received signal vector at the destination node and relay node can be expressed as follows:

$$\mathbf{y}^c_1 = \mathbf{H}^c_{sd}\mathbf{s}^c + \mathbf{z}^c_{d,1}, \tag{1}$$

$$\mathbf{y}^c_r = \mathbf{H}^c_{sr}\mathbf{s}^c + \mathbf{z}^c_{r,1}, \tag{2}$$

where $\mathbf{s}^c \in \mathbb{C}^{N\times 1}$, where s_i for $i = 1, 2, \ldots, N$ is the symbol transmitted from the i-th antenna of the source node; $\mathbf{z}^c_{r,1} \in \mathbb{C}^{N\times 1}$ and $\mathbf{z}^c_{d,1} \in \mathbb{C}^{N\times 1}$ represents the noise vector at the relay node and the destination node, respectively.

During the second time slot, the relay node processes the signal from the source node using either AF or DF methods. The signal received at the destination

node through the relay-aided transmission path can be described as follows

$$\mathbf{y}_2^c = \mathbf{H}_{rd}^c f_r(\mathbf{y}_r^c) + \mathbf{z}_{d,2}^c \tag{3}$$

where $f_r(\cdot)$ denotes the processing function applied to the vector $\mathbf{y}_r^c$ at the relay node prior to its transmission to the destination node; $\mathbf{z}_{d,2}^c \in \mathbb{C}^{N\times 1}$ represents the noise vector at the destination node.

The destination node has a combined receiving vector $\mathbf{y}^c = \begin{bmatrix}\mathbf{y}_1^c \\ \mathbf{y}_2^c\end{bmatrix}$. At the destination node, the transmitted signal is recovered using a linear detector according to the following equation

$$\hat{\mathbf{s}}^c = (\mathbf{W}^c)^H \mathbf{y}^c \tag{4}$$

where The weight matrix $\mathbf{W}^c$ is employed to detect the combined received signal $\mathbf{y}^c$. The estimated signal vector $\hat{\mathbf{s}}^c$ is compared to the transmitted signal vector $\mathbf{s}^c$ to calculate the BER.

3 The Proposed AE-Based Cooperative MIMO WBAN System

To meet the high reliability requirements of WBAN applications in healthcare systems and mitigate the effects of fading in the WBAN channel, we propose the use of cooperative MIMO systems employing AF and DF methods using AE techniques. Based on the study [42], we extend the solution using the AE technique for the cooperative MIMO-SDM communication system for the link S_2 to D with the aided relay node R_1. Accordingly, the system incorporates neural network layers representing a source node, a relay node, and a destination node. The weights and biases of neural network layers are determined through training using a labelled symbol set and channel state information with a known distribution. Furthermore, this study introduces two AE-based cooperative MIMO communication system structures using the AF and DF methods based on the bit-wise labelling method [38]. In this study, we represent mathematical expressions in the complex domain using a real-valued neural network with doubled size, i.e., two real values represent each complex number.

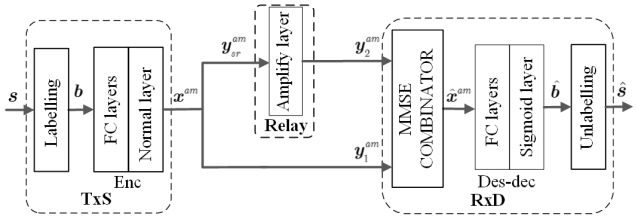

Figure 3. The AE-AF system using MMSE combinator.

3.1 The AF-Based Cooperative MIMO Systems Using AE Technology

In many WBAN applications, especially in health monitoring systems, communication reliability is a crucial parameter that affects the system's performane. Hence, in this section, we present two AF-based cooperative MIMO systems utilizing the AE technique for on-body communications, aimed at alleviating fading effects and enhancing BER performance with modest computational complexity. Based on the principle of operation of the cooperative MIMO system presented in Section 2, we introduce AF-based cooperative MIMO systems using AE technology with two different detectors at the destination node; those use the MMSE combinator (AE-AF-MMSE) and the combination of RTN networks (AE-AF-RTN) for WBAN.

3.1.1 The AE-AF System Using MMSE Combinator: As depicted in Figure 3, the AE-AF-MMSE consists of a source node (TxS), a relay node (Relay), and a destination node (RxD), respectively. At source node, the transmitted symbol vector $\mathbf{s}$ is bit-wise labelled as a vector $\mathbf{b}$ consisting of binary bits 0 and 1, $\mathbf{b} = [b_1, b_2, \ldots, b_P]^T$, with $P = N \times k$, $k = \log_2(M)$, M is order modulation. Table I represents an example of bit-wise labelling signals for the AE-AF-MMSE system with two transmitting antennas using BPSK modulation. The vector $\mathbf{b}$ is encoded into a transmitted signal vector as follows

$$\mathbf{x}^{am} = f_{\text{TxS}}(\mathbf{b}; \theta_{\text{TxS}}^{am}), \tag{5}$$

where $f_{\text{TxS}}(\cdot)$, θ_{TxS}^{am} denotes the processing function and the trainable parameters of the layers at the source node, respectively, the am index represents the AF method using the MMSE detector. The transmit vector $\mathbf{x}^{am}$ is power-normalized through the normalization layer in the encoder. A transmitted vector $\mathbf{x}^{am} = [x_1^{am}, x_2^{am}, \ldots, x_{2N}^{am}]^T$ be a real signal vector, includes $[x_1^{am}, \ldots, x_N^{am}]^T$ and $[x_{N+1}^{am}, \ldots, x_{2N}^{am}]^T$ represents the real part and the imaginary part of the complex signal vector, respectively. Each element of the vector $\mathbf{x}^{am}$ is a function of the label $\mathbf{b}$, $x_i^{am} = f_{TxS}(\mathbf{b}; \theta_{TxS,i}^{am})$, $i = 1, \cdots, 2N$, so the constellation on each transmitting antenna has $2^{k\times N}$ points. In the first time slot, the received signal vectors at the relay node and the destination node are given, respectively, as follows:

$$\mathbf{y}_{sr}^{am} = f_{chan}(\mathbf{H}_{sr}, \mathbf{x}^{am}, \mathbf{z}_{r,1}) = \mathbf{H}_{sr}\mathbf{x}^{am} + \mathbf{z}_{r,1}, \tag{6}$$

$$\mathbf{y}_1^{am} = f_{chan}(\mathbf{H}_{sd}, \mathbf{x}^{am}, \mathbf{z}_{d,1}) = \mathbf{H}_{sd}\mathbf{x}^{am} + \mathbf{z}_{d,1}, \tag{7}$$

where $f_{chan}(\cdot)$ is the transformation function at the channel layers, and this layer does not have any training parameters; the channel matrices and noise vectors are all represented by matrices and real-valued vectors, $\mathbf{H}_{sr} \in \mathbb{R}^{2N\times 2N}$, $\mathbf{H}_{sd} \in \mathbb{R}^{2N\times 2N}$, $\mathbf{z}_{r,1} \in \mathbb{R}^{2N\times 1}$, $\mathbf{z}_{d,1} \in \mathbb{R}^{2N\times 1}$. The relationship between complex channel matrices, noise vectors and real-value channel matrices, noise vectors as follows:

$$\mathbf{H}_{sr} = \begin{bmatrix}\text{Re}(\mathbf{H}_{sr}^c) & -\text{Im}(\mathbf{H}_{sr}^c) \\ \text{Im}(\mathbf{H}_{sr}^c) & \text{Re}(\mathbf{H}_{sr}^c)\end{bmatrix},$$

$$\mathbf{H}_{sd} = \begin{bmatrix}\text{Re}(\mathbf{H}_{sd}^c) & -\text{Im}(\mathbf{H}_{sd}^c) \\ \text{Im}(\mathbf{H}_{sd}^c) & \text{Re}(\mathbf{H}_{sd}^c)\end{bmatrix},$$

$$\mathbf{z}_{r,1} = \begin{bmatrix}\text{Re}(\mathbf{z}_{r,1}^c) \\ \text{Im}(\mathbf{z}_{r,1}^c)\end{bmatrix}, \mathbf{z}_{d,1} = \begin{bmatrix}\text{Re}(\mathbf{z}_{d,1}^c) \\ \text{Im}(\mathbf{z}_{d,1}^c)\end{bmatrix}.$$

The relay node amplifies the signal $\mathbf{y}_{sr}^{am}$ by utilizing the amplification matrix $\mathbf{F} \in \mathbb{R}^{2N\times 2N}$, where $\mathbf{F} = diag\{f_1, f_2, \ldots, f_{2N}\}$, and subsequently relays the amplified signal to the destination. In which, f_i, $(i = 1, 2, ..., 2N)$, is the amplification coefficient corresponding to the i-th neural of output layer of the relay node, f_i^c is calculated in [27] as follows

$$f_i = \sqrt{\frac{P_T}{N(\frac{P_T}{N}\|\mathbf{h}_{sr,i}\|^2 + 1)}}, \tag{8}$$

where P_T is the transmission power of the source node and the relay node, and the power transmitted on each antenna is normalized by using a factor of $1/N$. Vector $\mathbf{h}_{sr,i}$ represents the i-th row of the channel matrix from the source node to the relay node. In the second time slot, the destination node received signal vector from the relay path, denoted as $\mathbf{y}_2^{am}$, can be expressed as

$$\mathbf{y}_2^{am} = \mathbf{H}_{rd}\mathbf{F}\mathbf{y}_{sr}^{am} + \mathbf{z}_{d,2} = \mathbf{H}_{srd}\mathbf{x}^{am} + \tilde{\mathbf{z}}_2, \tag{9}$$

where $\mathbf{H}_{rd} = \begin{bmatrix} \mathrm{Re}(\mathbf{H}_{rd}^c) & -\mathrm{Im}(\mathbf{H}_{rd}^c) \\ \mathrm{Im}(\mathbf{H}_{rd}^c) & \mathrm{Re}(\mathbf{H}_{rd}^c) \end{bmatrix}$; $\mathbf{z}_{d,2} = \begin{bmatrix} \mathrm{Re}(\mathbf{z}_{d,2}^c) \\ \mathrm{Im}(\mathbf{z}_{d,2}^c) \end{bmatrix}$; $\mathbf{H}_{srd} = \mathbf{H}_{rd}\mathbf{F}\mathbf{H}_{sr}$ and $\tilde{\mathbf{z}}_2 = \mathbf{H}_{rd}\mathbf{F}\mathbf{z}_{d,2}$. The vector of combined signals at the destination node is represented as follows

$$\begin{bmatrix} \mathbf{y}_1^{am} \\ \mathbf{y}_2^{am} \end{bmatrix} = \begin{bmatrix} \mathbf{H}_{sd} \\ \mathbf{H}_{srd} \end{bmatrix} \mathbf{x}^{am} + \begin{bmatrix} \mathbf{z}_1 \\ \tilde{\mathbf{z}}_2 \end{bmatrix}. \tag{10}$$

Destination node recover the signal vector $\hat{\mathbf{x}}^{am}$, as follows

$$\hat{\mathbf{x}}^{am} = (\mathbf{W}^{am})^H \mathbf{y}^{am}, \tag{11}$$

where $\mathbf{W}^{am}$ is the weight matrix of the MMSE combination calculated as follows [27]

$$\mathbf{W}^{am} = (\mathbf{R}_a)^{-1}\mathbf{R}_c, \tag{12}$$

where $\mathbf{R}_c = \frac{P_T}{N}\begin{bmatrix} \mathbf{H}_{sd} \\ \mathbf{H}_{srd} \end{bmatrix}$, $\mathbf{R}_a = \begin{bmatrix} \mathbf{A} & \mathbf{0} \\ \mathbf{0} & \mathbf{B} \end{bmatrix}$, $\mathbf{A}$ and $\mathbf{B}$ are respectively calculated as follows:

$$\mathbf{A} = \frac{P_T}{N}\mathbf{H}_{sd}(\mathbf{H}_{sd})^H + \sigma_{z,1}^2\mathbf{I}_{2N}$$

$$\mathbf{B} = \frac{P_T}{N}\mathbf{H}_{srd}(\mathbf{H}_{srd})^H + \sigma_r^2\mathbf{H}_{rd}(\mathbf{F})^2(\mathbf{H}_{rd})^H + \sigma_{z,2}^2\mathbf{I}_{2N}$$

The label vector is recovered $\hat{\mathbf{b}}^{am}$ at the destination node (RxD)

$$\hat{\mathbf{b}}^{am} = f_{\mathrm{RxD}}(\hat{\mathbf{x}}^{am}; \theta_{\mathrm{dec}}^{des,am}), \tag{13}$$

where $f_{\mathrm{RxD}}(\cdot)$, $\theta_{\mathrm{dec}}^{des,am}$ represents the processing function and the trainable parameters of the decoder network, respectively. The MMSE weight matrix $\mathbf{W}^{am}$ in equation (12) can be split into two matrices, $\mathbf{W}_1^{am}$ and $\mathbf{W}_2^{am}$, representing the weight matrix of the direct transmission signal and the weight matrix of the forward path, respectively, precisely

$$\mathbf{W}^{am} = \begin{bmatrix} \mathbf{W}_1^{am} \\ \mathbf{W}_2^{am} \end{bmatrix}, \tag{14}$$

where $\mathbf{W}_1^{am}$ and $\mathbf{W}_2^{am}$ matrices, can be calculated as follows [27]:

$$\mathbf{W}_1^{am} = \left[\mathbf{A}\right]^{-1}\frac{P_T}{N}\mathbf{H}_{sd}, \tag{15}$$

$$\mathbf{W}_2^{am} = \left[\mathbf{B}\right]^{-1}\frac{P_T}{N}\mathbf{H}_{srd}. \tag{16}$$

However, in some cases, due to the influence of activities and the positioning of the WBAN user, the source node on the right wrist cannot transmit directly to the destination node on the left waist. In such scenarios, the system maintains communication through a relay path or cooperates with additional relays to transmit data to the destination node using MMSE weight matrices, similar to equations (14), (15), and (16). The number of network layers, activation functions, and number of output nodes per layer of the AE-AF-MMSE system are listed in Table II.

Table I
Transmitted Symbol Streams Are Mapped Bit-wise Labelling Vectors

$\mathbf{s} = [s_1, s_2]$	00	01	10	11
$\mathbf{b} = [b_1, b_2]$	00	01	10	11

Table II
The Structure of the AE-AF System Using MMSE Combinator

	Layer × layer No.	Activation function	Output neurons
Source node (TxS)			
Encoder (Enc)	input	-	P
	FC × 3	relu	64
	FC	linear	$2N$
	Normalization	-	$2N$
Channel	Rayleigh	-	$2N$
	Noise	-	$2N$
Relay	Amplify	-	$2N$
Destination node (RxD)			
Combinator	MMSE	-	$2N$
Decoder (Dec)	FC × 3	relu	64
	FC	sigmoid	P

The source node consists of an input layer and hidden layers, which utilize fully connected (FC) layers with the activation functions of relu/linear. The last layer performs power normalization. The channel layer and relay nodes have no training parameters. The destination node includes an MMSE detector and a decoder (Dec). The decoder employs FC layers with the activation functions of relu/linear, while the output layer of the decoder utilizes the sigmoid function as its activation function.

3.1.2 The AE-AF System Using the RTN Combinator: The impact of radio transmission channels leads to a decrease in the performance of communication systems. Hence, in several studies [11, 36], communication systems based on Autoencoder (AE) propose the adoption of a Radio Transformer Network (RTN) served the purpose of channel estimation and mitigating the

impact of fading channels to enhance the system's overall performance. Furthermore, AE-based MIMO systems, which suggested utilizing an RTN network as a detector, significantly outperform conventional MIMO systems in work [42].

Hence, we suggest incorporating RTN networks as a combinator of the AE-AF system (AE-AF-RTN). While the weight matrix of MMSE combinator $\mathbf{W}$ is determined using the equation (12), the weights and biases of RTN are automatically learned and updated during a training phase by minimizing the binary cross-entropy loss. The destination node structure of the AE-AF-RTN is represented in Figure 4.

At the first time slot, the signals received at the destination node and the relay node, y_1^{ar} and y_{sr}^{ar}, respectively, are calculated similarly to (6) and (7), the *ar* index represents the AF method using the RTN combinator. Within this system, the relay node utilizes the normalization layer to normalize the power of y_{sr}^{ar} and transmits it to the destination node during the second time slot. The relay signal received at the destination node can be described as follows

$$\mathbf{y}_2^{ar} = \mathbf{H}_{rd} f_{\text{nor}}^{r}(\mathbf{y}_{sr}^{ar}) + \mathbf{z}_{d,2} \tag{17}$$

where the function $f_{\text{nor}}^{r}(\cdot)$ is the normalization function at the relay node. It is important to note that the relay node has no training parameters.

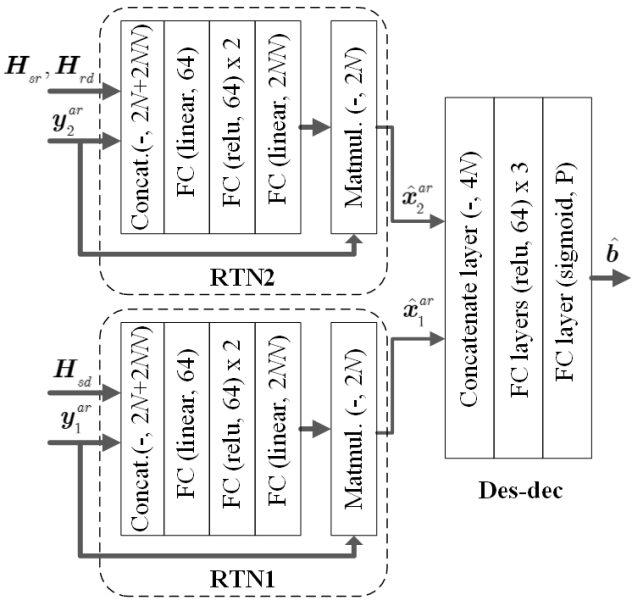

Figure 4. The destination node structure of the AE-AF-RTN system.

The RTN1 and RTN2 networks estimate signals $\hat{\mathbf{x}}_1^{ar}$ and $\hat{\mathbf{x}}_2^{ar}$ from received signals $\mathbf{y}_1^{ar}$ and $\mathbf{y}_2^{ar}$, respectively, as follows:

$$\hat{\mathbf{x}}_1^{ar} = f_{rtn1}(\mathbf{y}_1^{ar}, \mathbf{H}_{sd}; \theta_{\text{rtn1}}^{ar})\mathbf{y}_1^{ar}, \tag{18}$$

$$\hat{\mathbf{x}}_2^{ar} = f_{\text{rtn2}}(\mathbf{y}_2^{ar}, \mathbf{H}_{sr}, \mathbf{H}_{rd}; \theta_{\text{rtn2}}^{ar})\mathbf{y}_2^{ar}, \tag{19}$$

where $f_{\text{rtn1}}(\cdot)$, $f_{\text{rtn2}}(\cdot)$, $\theta_{\text{rtn1}}^{ar}$, $\theta_{\text{rtn2}}^{ar}$ denote the processing function and the trainable parameters of the RTN1 and RTN2 networks, respectively. The estimated signals $\hat{\mathbf{x}}_1^{ar}$ and $\hat{\mathbf{x}}_2^{ar}$ are simultaneously inputted into the decoder via the concatenate layer, and the label $\hat{\mathbf{b}}^{ar}$ is estimated:

$$\hat{\mathbf{b}}^{ar} = f_{\text{dec}}(\hat{\mathbf{x}}_1^{ar}, \hat{\mathbf{x}}_2^{ar}; \theta_{\text{dec}}^{des,ar}), \tag{20}$$

where $f_{\text{dec}}(\cdot)$, $\theta_{\text{dec}}^{des,ar}$ denote the processing function and the trainable parameters of the decoder network at the destination node, respectively.

3.1.3 Training Procedure of AE-AF Systems: The AE-AF systems are trained using a dataset that includes transmitted symbols, noise at the receiver and channel state information, denoted as $\mathbf{s}$, $\mathbf{z} = \{\mathbf{z}_{r,1}, \mathbf{z}_{d,1}, \mathbf{z}_{d,2}\}$, and $\mathbf{H} = \{\mathbf{H}_{sd}, \mathbf{H}_{sr}, \mathbf{H}_{rd}\}$. A set of M-ary modulated symbols $\mathbf{s}$ is randomly generated and labelled by the bit-wise method as a vector $\mathbf{b}$, fed into the source node's encoder. To achieve the best performance for the system, the dataset for channel, $\mathbf{z}$ and $\mathbf{H}$, should closely resemble the practical realizations, ideally measured on an actual channel [46], [37]. However, these methods require collecting data in various user activity conditions, and the data collection time needs to be sufficiently long. Therefore, to facilitate the evaluation of the proposed solution in research, datasets are often generated using Python simulation. The realizations of $\mathbf{H}$ is generated with a Rayleigh distribution, and the dataset $\mathbf{z}$ consists of Gaussian random variables with a variance of σ^2 and a mean value of 0. In addition, $\mathbf{H}$ and $\mathbf{z}$ are fed into the transmission channel layer. The AE-AF systems employ a bit-labelling approach that incorporates the use of the BCE loss function [33]

$$L_{\text{BCE}} = -\frac{1}{B}\sum_{q=1}^{B}\sum_{p=1}^{P}(b_{q,p}\log\hat{b}_{q,p} + (1-b_{q,p})\log(1-\hat{b}_{q,p})), \tag{21}$$

where $b_{q,p}$ denotes the q-th element of label vector and the p-th label vector of the batch size B; $\hat{b}_{q,p}$ denotes estimated label vector. The Stochastic Gradient Descent (SGD) approache is most popular algorithms for locating optimal parameter sets, θ_{AE}, and the backpropagation method is employed to calculate the gradient [33]. The parameter set $\theta_{\text{AE}} = (\theta_{\text{TxS}}, \theta_{\text{RxD}})$ is updated iteratively in SGD as follows

$$\theta_{\text{AE}}^{n+1} = \theta_{\text{AE}}^{n} - \eta\frac{\partial L_{\text{BCE}}^{n}}{\partial\theta_{\text{AE}}^{n}}, \tag{22}$$

where η, $\frac{\partial L_{\text{BCE}}^{n}}{\partial\theta_{\text{AE}}^{n}}$ denote learning rate, gradient operator of the n-th iteration, respectively.

The training process stops when the system meets one of two conditions, either reaching a threshold value for the loss function (L_{BCE}^{th}) or completing a specified number of iterations (N_{iter}). Upon completion of the training process, the training parameters from the transmitter to the receiver are synchronously optimized. The relay node of the AE-AF system amplifies and forwards signals to the destination node, lacking any training parameters. Consequently, only a single training phase is required for the entire system, as described in Algorithm 1. In which SNR is the range of values of the ratio between signal power and noise power; θ_{TxS}^{af} is the training parameters of source node, the af index represents the AF method; $\theta_{\text{RxD}}^{am} = \theta_{\text{dec}}^{des,am}$

and $\theta^{ar}_{\text{RxD}} = (\theta^{ar}_{\text{rtn1}}, \theta^{ar}_{\text{rtn2}}, \theta^{des,ar}_{\text{dec}})$ respectively represent the receiver nodes' parameters in the AE-AF-MMSE and AE-AF-RTN systems, as abbreviated θ^{af}_{RxD} for both systems.

Algorithm 1 Training AE-AF systems.

Input: $\mathbf{b}, \mathbf{H}, \mathbf{z}$, SNR, L^{th}_{BCE}, N_{iter}.
1 : $count = 0$
2 : **While** $count \leq N_{iter}$:
3 : **for** k **in** range (SNR):
4 : Train AE-AF$_{srd}$, calculate L_{BCE}
5 : $L_{BCE} = \text{AE-AF}_{srd}.\ \text{train}\Big(\text{in} = \Big[\mathbf{b}, \mathbf{H}, \mathbf{z}; \theta^{af}_{\text{TxS}}, \theta^{af}_{\text{RxD}}\Big], \text{out} = \Big[\hat{\mathbf{b}}\Big]\Big)$
6 : **end for**
7 : **if** $L_{BCE} \leq L^{th}_{BCE}$:
8 : **break**
9 : **end if**
10 : $count+ = 1$
11 : **end While**
Output: Trained parameters: $\theta^{af}_{\text{TxS}}, \theta^{af}_{\text{RxD}}$

3.2 The DF-Based Cooperative MIMO Systems Using AE Technology

To further enhance performance for on-body communicaiton, we propose DF-based cooperative MIMO systems using the AE technique with the MMSE combinator and the RTN combinator, abbreviated AE-DF-MMSE and AE-DF-RTN, respectively. The AE-DF systems offer improved BER performance, but it comes at the cost of a significant increase in computational complexity compared to AE-AF systems.

3.2.1 The AE-DF System Using MMSE Combinator: The AE-DF-MMSE system consists of a source node (TxS), a destination node (RxD), and a relay node; the relay node comprises a receiver (RxR) and a transmitter (TxR), as depicted in Figure 5. The encoder encodes the bit-wise labelled vector $\mathbf{b}$ into the transmitted signal vector $\mathbf{x}^{dm}$ according to equation (5) with the dm index denotes the DF method using the MMSE combinator.

During the first time slot, the source node simultaneously transmits the signal vector $\mathbf{x}^{dm}$ to both the relay and destination nodes. Equations (6) and (7) respectively represent the received signal vectors $\mathbf{y}^{dm}_{sr}$ at the relay node and $\mathbf{y}^{dm}_{1}$ at the destination node.

During the second time slot, the source node ceases transmission, and the relay node utilizes the MMSE detector to estimate the transmitted signal $\hat{\mathbf{b}}^{dm}_{r}$, as outlined below

$$\hat{\mathbf{b}}^{dm}_{r} = f_{\text{RxR}}(\mathbf{W}^{H}_{r}\mathbf{y}^{dm}_{sr}; \theta^{dm}_{\text{RxR}}), \tag{23}$$

where $f_{\text{RxR}}(\cdot)$, θ^{dm}_{RxR} denote the proccesing function and the trainable parameters of the decoder at the relay node, respectively; $\mathbf{W}^{H}_{r}$ is the MMSE detection matrix calculated using the expression:

$$\mathbf{W}_{r} = \left[\frac{P_T}{N}\mathbf{H}_{sr}(\mathbf{H}_{sr})^{H} + \sigma^2_{r,1}\mathbf{I}_{2N}\right]^{-1}\frac{P_T}{N}\mathbf{H}_{sr}. \tag{24}$$

Then, the encoder of the relay node (TxR) encodes $\hat{\mathbf{b}}^{dm}_{r}$ into the signal vector $\mathbf{x}^{dm}_{r}$ as follows

$$\mathbf{x}^{dm}_{r} = f_{\text{TxR}}(\hat{\mathbf{b}}^{dm}_{r}; \theta^{dm}_{\text{TxR}}), \tag{25}$$

where $f_{\text{TxR}}(\cdot)$, θ^{dm}_{TxR} denote the processing function of layers and the trainable parameters of TxR, respectively.

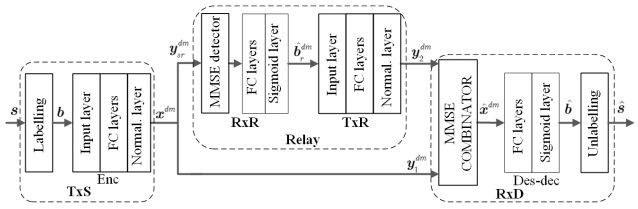

Figure 5. The AE-DF system using MMSE combinator.

Afterwards, the vector $\mathbf{x}^{dm}_{r}$ is transmitted to the destination node. The relay signal vector received at the destination node is given by

$$\mathbf{y}^{dm}_{2} = f_{chan}(\mathbf{H}_{rd}, \mathbf{x}^{dm}_{r}, \mathbf{z}_{d,2}) = \mathbf{H}_{rd}\mathbf{x}^{dm}_{r} + \mathbf{z}_{d,2}. \tag{26}$$

The destination node combines two received signal vectors $\mathbf{y}^{dm}_{1}$ and $\mathbf{y}^{dm}_{2}$, then estimated signal vector is

$$\hat{\mathbf{x}}^{dm} = (\mathbf{W}^{dm})^{H}\mathbf{y}^{dm}, \tag{27}$$

where $\mathbf{W}^{dm} = \begin{bmatrix}\mathbf{W}^{dm}_{1}\\ \mathbf{W}^{dm}_{2}\end{bmatrix}$, the weight matrices $\mathbf{W}^{dm}_{1}$ and $\mathbf{W}^{dm}_{2}$ are the weight matrix detector for direct and forwarding paths, calculated as follows:

$$\mathbf{W}^{dm}_{1} = \left[\frac{P_T}{N}\mathbf{H}_{sd}(\mathbf{H}_{sd})^{H} + \sigma^2_{d,1}\mathbf{I}_{2N}\right]^{-1}\frac{P_T}{N}\mathbf{H}_{sd}, \tag{28}$$

$$\mathbf{W}^{dm}_{2} = \left[\frac{P_T}{N}\mathbf{H}_{rd}(\mathbf{H}_{rd})^{H} + \sigma^2_{d,2}\mathbf{I}_{2N}\right]^{-1}\frac{P_T}{N}\mathbf{H}_{rd}. \tag{29}$$

Vector label estimated $\hat{\mathbf{b}}$ at the destination node is given by

$$\hat{\mathbf{b}} = f_{\text{RxD}}((\mathbf{W}^{dm})^{H}\mathbf{y}^{dm}; \theta^{dm}_{\text{RxD}}) = f_{\text{RxD}}(\hat{\mathbf{x}}^{dm}; \theta^{dm}_{\text{RxD}}). \tag{30}$$

Vector $\hat{\mathbf{b}}$ is unlabelled to obtain estimated vector $\hat{\mathbf{s}}$. The structural configurations of the source node and destination node in the AE-DF-MMSE system are analogous to those of the AE-AF-MMSE system, as presented in Table II. The difference from the AE-AF-MMSE system is that the relay node of the AE-DF-MMSE includes a receiver and a transmitter. The structure of this relay node is listed in Table III.

3.2.2 The AE-DF System Using RTN Combinator: Like the AE-DF-MMSE system, the AE-DF-RTN system employs two time slots for transmitting signals from the source node to the destination node, involving both direct and transmission through a relay node, as depicted in Figure 5. At the relay node, the received signal is decoded by the relay node, then re-encoded and forwarded to the destination node.

During the first time slot, the received signal vectors at the relay node ($\mathbf{y}^{dr}_{sr}$) and the destination node ($\mathbf{y}^{dr}_{1}$) can be expressed using equations (6) and (7), respectively, with the dr index represents the DF method using the RTN detector. The difference between the AE-

Table III
THE STRUCTURE OF THE RELAY NODE

	Layer × layer No.	Activation function	Output neurons
Relay receiver (RxR)			
Detector	MMSE	-	$2N$
Decoder (dec)	FC × 3	relu	64
	FC	sigmoid	P
Relay transmitter (TxR)			
Encoder (enc)	input	-	P
	FC × 3	relu	64
	FC	linear	$2N$
	Normalization	-	$2N$

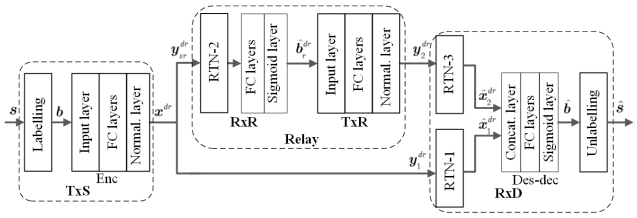

Figure 6. The AE-DF system using RTN combinator.

DF-RTN system and the AE-DF-MMSE system is that the MMSE detectors at the relay and destination nodes are replaced with RTN networks.

In the second time slot, the vector label $\hat{\mathbf{b}}_r^{dr}$ is estimated

$$\hat{\mathbf{b}}_r^{dr} = f_{\text{dec}}^{re}\big(f_{\text{rtn2}}(\mathbf{y}_{sr}^{dr}, \mathbf{H}_{sr}; \theta_{\text{rtn2}}^{dr})\mathbf{y}_{sr}^{dr}; \theta_{\text{dec}}^{re,dr}\big), \quad (31)$$

where $f_{\text{rtn2}}(\cdot)$, $f_{\text{dec}}^{re}(\cdot)$, $\theta_{\text{rtn2}}^{dr}$, $\theta_{\text{dec}}^{re,dr}$ denote the processing functions and trainable parameters of the RTN2 network and decoder at the relay node, respectively. Then, the encoder of the relay node encode vector $\hat{\mathbf{b}}_r^{dr}$, as follows

$$\mathbf{x}_r^{dr} = f_{\text{TxR}}(\hat{\mathbf{b}}_r^{dr}; \theta_{\text{TxR}}^{dr}). \quad (32)$$

At the destination node, the estimated signals are received via both the direct path and the relay path, as given by:

$$\hat{\mathbf{x}}_1^{dr} = f_{\text{rtn1}}(\mathbf{y}_1^{dr}, \mathbf{H}_{sd}; \theta_{\text{rtn1}}^{dr})\mathbf{y}_1^{dr}, \quad (33)$$

$$\hat{\mathbf{x}}_2^{dr} = f_{\text{rtn3}}(\mathbf{y}_2^{dr}, \mathbf{H}_{rd}; \theta_{\text{rtn3}}^{dr})\mathbf{y}_2^{dr}, \quad (34)$$

where $f_{\text{rtn1}}(\cdot)$, $f_{\text{rtn3}}(\cdot)$, $\theta_{\text{rtn1}}^{dr}$, $\theta_{\text{rtn3}}^{dr}$ denote the processing functions and trainable parameters of the RTN1 and the RTN3 networks at the destination node, respectively. The signal vectors $\hat{\mathbf{x}}_1^{dr}$ and $\hat{\mathbf{x}}_2^{dr}$ are decoded by the decoder of the destination node and unlabelled to obtain the estimated vector $\hat{\mathbf{s}}$:

$$\hat{\mathbf{s}} = \text{Unlabelling}(f_{\text{dec}}^{des}(\hat{\mathbf{x}}_1^{dr}, \hat{\mathbf{x}}_2^{dr}; \theta_{\text{dec}}^{des,dr})). \quad (35)$$

3.2.3 Training Procedure of AE-DF Systems: The AE-DF systems are trained using a dataset that includes transmitted symbols, noise at the receiver and channel state information, denoted as $\mathbf{s}$, $\mathbf{z} = \{\mathbf{z}_{r,1}, \mathbf{z}_{d,1}, \mathbf{z}_{d,2}\}$, and $\mathbf{H} = \{\mathbf{H}_{sd}, \mathbf{H}_{sr}, \mathbf{H}_{rd}\}$. A set of M-ary modulated symbols $\mathbf{s}$ is randomly generated and labelled by the bit-wise method as a vector $\mathbf{b}$, fed into the source node's encoder. To attain the optimum performance for the system, the channel datasets, $\mathbf{z}$ and $\mathbf{H}$, should closely mirror the practical realizations, ideally measured on a real-world channel. However, to ease the evaluation of the suggested approach, datasets, $\mathbf{H}$ and $\mathbf{z}$, with Rayleigh and Gaussian distributions, respectively, are generated using Python simulation. In addition, $\mathbf{H}$ and $\mathbf{z}$ are fed into the transmission channel layer. The AE-DF systems, which include a direct path and a relay path, are trained in two sequential phases. However, when the system only consists of relay paths, the system only needs to be trained in a single phase, as in Algorithm 1.

The training phases minimize the function loss BCE, as in equation (21), and the training parameters are updated according to equation (22) for the SGD method. The phase training process stops when the system meets one of two conditions: either the value of the loss variable reaches a threshold value or the number of training iterations reaches a predetermined value. When the training process ends, the system's parameters are optimized synchronously from the source node through the relay node to the destination node.

The relay node of the AE-DF system decodes the received signal and then re-encodes it for transmission to the destination node with two training parameters, θ_{RxR} and θ_{TxR}. Additionally, the study [36] suggests that the AE-based cooperative system, employing the DF method, undergoes training in a single phase, resulting in suboptimal performance due to the lack of information about the estimated signal at the relay node $\hat{\mathbf{b}}_r$. Therefore, to attain optimal performance, we suggest a two-phase sequential training approach for the AE-DF system: the first phase optimizes training from TxS to RxR, and the second phase encompasses training for the entire system, as described in Algorithm 2. The parameters and variables of the AE-DF systems are as follows:

- SNR is the range of values of the ratio between signal and noise powers;
- N_{iter} is the number of training;
- L_{BCE1}^{th} and L_{BCE2}^{th} are the threshold values of L_{BCE1} and L_{BCE2}, respectively;
- θ_{TxS}^{df} is the training parameter set of source node of AE-DF system;
- $\theta_{\text{RxR}}^{dm} = \theta_{\text{dec}}^{re,dm}$ and $\theta_{\text{RxR}}^{dr} = (\theta_{\text{rtn2}}^{dr}, \theta_{\text{dec}}^{re,dr})$ respectively represent the parameter set of the relay node's receiver of the AE-DF-MMSE system and AE-DF-RTN system, as abbreviated θ_{RxR}^{df} for both systems;
- θ_{TxR}^{df} is the transmtter's training parameter set of relay node;
- $\theta_{\text{RxD}}^{dr} = (\theta_{\text{rtn1}}^{dr}, \theta_{\text{rtn3}}^{dr}, \theta_{\text{dec}}^{des,dr})$ and $\theta_{\text{RxD}}^{dm} = \theta_{\text{dec}}^{des,dm}$ respectively represent the destination node's parameters of the AE-DF-MMSE system and AE-DF-RTN system, as abbreviated θ_{RxD}^{df} for both systems.

During the first training phase, the AE-DF system focuses on training the relay path, which includes a source node, a receiver of relay node. In the second training phase, We train the entire system, both the relay and direct paths synchronously.

Algorithm 2 Training AE-DF system.

Input: $\mathbf{b}, \mathbf{H}, \mathbf{z}$, SNR, L^{th}_{BCE1}, L^{th}_{BCE2}, N_{iter}.
1 : $count = 0$
2 : **While** $count \leq N_{iter}$:
3 : **for** k **in** range (SNR):
4 : *Phase 1:* Train AE-DF$_{sr}$, calculate L_{BCE1}
5 : **if** $L_{BCE1} > L^{th}_{BCE1}$:
6 : $L_{BCE1} = \text{AE-DF}_{sr}.\ \text{train}\Big(\text{in} = \Big[\mathbf{b}, \mathbf{H}_{sr}, \mathbf{z}_{r,1}; \theta^{df}_{\text{TxS}}, \theta^{df}_{\text{RxR}}\Big], \text{out} = \Big[\hat{\mathbf{b}}_r\Big]\Big)$
7 : **end if**
8 : *Phase 2:* Train AE-DF$_{srd}$, calculate L_{BCE2}
9 : $L_{BCE2} = \text{AE-DF}_{srd}.\ \text{train}\Big(\text{in} = \Big[\mathbf{b}, \mathbf{H}, \mathbf{z}; \theta^{df}_{\text{TxS}}, \theta^{df}_{\text{RxR}}, \theta^{df}_{\text{TxR}}, \theta^{df}_{\text{RxD}}\Big], \text{out} = \Big[\hat{\mathbf{b}}\Big]\Big)$
10 : **end for**
11 : **if** $L_{BCE2} \leq L^{th}_{BCE2}$:
12 : **break**
13 : **end if**
14 : $count += 1$
15 : **end While**
Output: Trained parameters: $\theta^{df}_{\text{TxS}}, \theta^{df}_{\text{RxR}}, \theta^{df}_{\text{TxR}}, \theta^{df}_{\text{RxD}}$

Cooperative DF systems are more complex than AF systems because they detect and re-modulate at the relay node. Nevertheless, DF systems outperform AF systems because they can avoid amplifying noise in the relay path. Some simulation results in Section 4 illustrate the improvement in DF systems achieved in specific cases.

4 Simulation Results

This section focuses on simulating and evaluating the BER performance of the AE-based cooperative MIMO system in WBAN to mitigate the effects of multi-path propagation and enhance link's reliability. The transmission channel for the WBAN depends on the placement of the sensors on the human body. Many channel models have been proposed for intra-WBAN networks in specific cases, such as the Lognormal, Weibull, Rice, and Rayleigh distributions [47–49]. The Rice and Rayleigh distributions are suitable for narrow-band MICS and ISM in environments with multiple scattering and reflections. In this research scope, we employ a Rayleigh channel for simulating and evaluating the performance of cooperative MIMO systems on the body. This channel model represents the most challenging scenario among fading channels [50], when the proposed system performs effectively on the Rayleigh channel, it is expected to perform well on all other channels.

Furthermore, the system utilizes BPSK modulation for two-hop communication links supported by the IEEE 802.15.6 standard. The performance of the proposed AE-AF systems is compared to the performance of AF-based MIMO systems using the MMSE combinator proposed in the study [27], referred to as baselines called AF-MMSE. Additionally, the performance of the proposed AE-DF system is compared to the performance of the DF-based MIMO system using the ZF combinator (DF-ZF) in the study [29] and the MMSE combinator (DF-MMSE), which are referred to as baselines. The baseline BER performance curves are simulated using MATLAB R2019b software.

The single-hop communication link (from S_1 to D) can utilize the AE-based MIMO schemes (AE-MIMO), as presented in the study [42]. Furthermore, the performance of the AE-MIMO system also establishes a baseline for comparing the performance of the proposed cooperative AE-AF and AE-DF systems. The performance of the proposed systems is simulated utilizing Python 3.6 software accompanied by the Tensorflow 1.14 and Keras 2.0 libraries. All source, relay, and destination nodes are equipped with equal antennas. Furthermore, the transmit power is normalized to 1 across the N antennas. For training the proposed systems, we employ the SGD with Adam optimizer [51] having a learning rate of 0.001. The batch size B is set to 256 in most cases, and the training process is conducted over 50,000 epochs. Additionally, we consider an SNR range from 5 dB to 25 dB with a 5 dB interval. Depending on each system, the threshold values are determined based on experience. The BER of the baseline and proposed systems is simulated and evaluated over 10^4 frames, each containing 100 symbols.

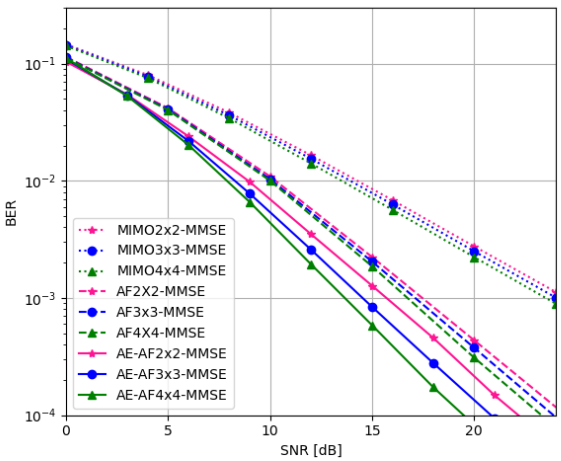

Figure 7. BER comparison between AE-AF-MMSE and the conventional AF-MMSE for $N = 2, 3, 4$.

First, we simulate the proposed systems in the scenario where the signal is transmitted from the source node to the destination node through a direct and a relay paths. The performance of the AE-AF-MMSE, AE-AF-RTN, AE-DF-MMSE, and AE-DF-RTN systems is depicted in Figures 7, 8, 10 and 11, respectively.

Figure 7 compares the BER performance of the AE-AF-MMSE system and the AF-MMSE system [27], the conventional MIMO using MMSE detector system with $N = 2, 3, 4$, the L^{th}_{BCE} threshold value of these systems is equal to 10^{-6}. Specifically, with $N = 2$, the BER performance of the AE-AF-MMSE system allows for an 8 dB

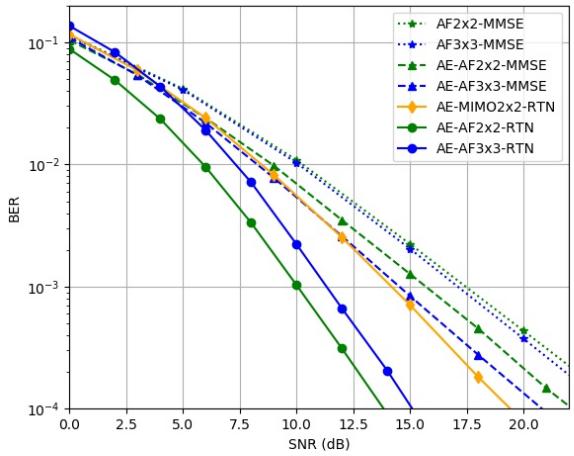

Figure 8. BER comparison between AE-AF-RTN and AE-AF-MMSE systems with N = 2, 3.

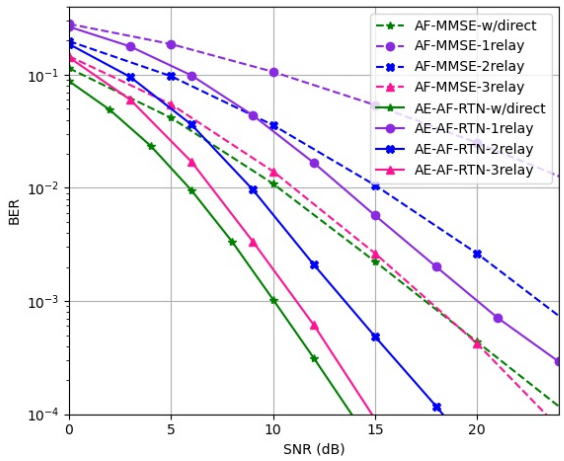

Figure 9. BER comparison between AE-AF-RTN and the conventional AF-MMSE with N = 2 and L = 1, 2, 3.

gain compared to the BER performance of the MIMO-MMSE system at a BER of 10^{-3}. Meanwhile, compared to the AF-MMSE system, the proposed system allows for respective improvements of 2 dB and 3 dB when using 2 and 4 antennas at BER = 10^{-3}.

Next, we simulate and compare the BER performance of the AE-AF-RTN and AE-AF-MMSE systems with N = 2, 3 as shown in Figure 8. The BER curves of the AE-AF-RTN system exhibit steeper slopes compared to the AF-MMSE, AE-AF-MMSE, and AE-MIMO systems, indicating that AE-AF-RTN achieves higher diversity gain than the other systems. The BER performance of the AE-AF-RTN system is compared to the AE-MIMO-RTN [42], AE-AF-MMSE and AF-MMSE systems. With N = 2, the BER performance of the AE-AF-RTN system improves by 4 dB, 5.5 dB and 7.5 dB compared to AE-MIMO-RTN, AE-AF-MMSE and AF-MMSE systems, respectively, at the BER of 10^{-3}. Similarly, at BER = 10^{-3}, the AE-AF-RTN system outperforms AE-AF-MMSE and AF-MMSE systems with gains of 3.5 dB and 6 dB, respectively, when all systems are equipped with three transceive antennas. However, the quantity of points in the constellations increases quickly as AE-AF-RTN increases the number of transmit antennas. As a result, when the system encounters interferences such low SNR and fading channels, there are more mistakes in estimated signals at the receiver, which causes a rapid fall in system performance. Additionally, we note that whereas the weight matrix of the MMSE combinator in the base system and the proposed AE-AF-MMSE system are computed based on specific SNR values, as in equal (12), the learning parameters of the RTN combinator in the AE-AF-RTN system are automatically learnt through training over a range of SNRs. Therefore, the simulation results show that the BERs of AE-AF-MMSE and AF-MMSE with $N = 3$ are better than with $N = 2$, while the BERs of AE-AF-RTN with $N = 3$ are worse than with $N = 2$. simultaneously, at a low SNR range (SNR < 5 dB), the performance of AE-AF-RTN with $N = 3$ is poorer than the other two systems.

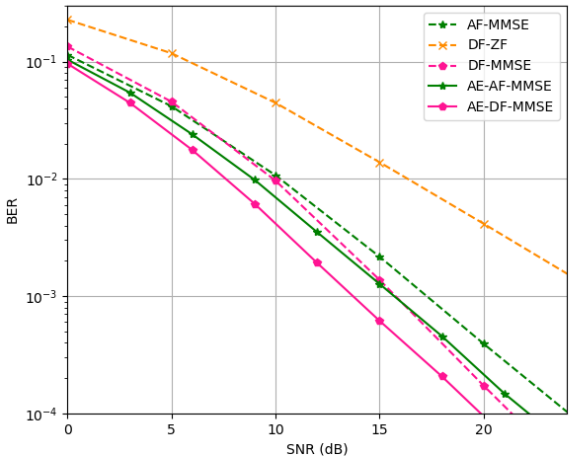

Figure 10. BER comparison between AE-DF-MMSE and DF-MMSE with N = 2.

When the direct transmision is severely affected by extensive propagation loss due to the influence of activities and the position of the WBAN user, the signal from the source to the destination can only rely on the assistance of one or several relay nodes. In this scenario, the BER performance of the proposed systems, AE-AF-RTN and AE-DF-RTN, is illustrated in Figures 9 and 12, respectively.

We simulate the AE-AF-RTN system with N = 2, where the system communicates through L relay paths with and without direct path. With L = 1, 2, 3, the BER performance of the proposed system is compared with that of the AF-MMSE system, as shown in Figure 9. The BER curves of the AE-AF-RTN systems exhibit steeper slopes compared to the BER curves of the AF-MMSE systems in cases with and without a direct link. This indicates that the proposed systems using AE technique achieve higher diversity gain compared to baseline systems that do not use AE technique. With L = 1, meaning the system only uses a relay path, abbreviated as *1relay*, the BER of the system using RTN improves by about 10 dB compared to the AE-AF-MMSE at BER = 2.10^{-2} and $L^{th}_{BCE} = 2.10^{-3}$. However, the performance of this system saturates at BER = 10^{-3} because we chose a relatively small training batch size, $B = 256$, while the proposed system requires training with a

larger batch size to achieve optimal performance. When the systems use 2 and 3 relay paths, abbreviated as *2relay* and *3relay*, respectively, $L_{BCE}^{th} = 10^{-4}$, the proposed system improves by 9.5 dB and 6.5 dB at BER = 10^{-3}, respectively, compared to the AF-MMSE system. The AE-AF-RTN cooperative system with *3relay* achieves a BER performance close to that of the system using one direct path and one relay path. When the systems have the number of relay paths $L = 1, 2, 3$, respectively, the BER curve gradually decreases, which means the performance of the systems improves. However, the system will have to pay the cost of computational complexity and energy consumption. Assuming that the transmission power of the source node and relay nodes is normalized to 1, the system's power consumption will increase as the number of relay nodes increases. Table IV lists the total transmission power of the system in various simulation scenarios. It is clear that the cooperative system with one direct transmission path and one relay path, which provides the best BER performance and the lowest power consumption, is the best-case situation. In the specific case where there is no direct path, depending on the requirements of each application, we choose the system configuration with the most suitable value of L.

Table IV
Total Power Consumption of Both Baseline and the Proposed Systems in Different Cases

	w/direct	**1relay**	**2relay**	**3relay**
Number of Node	1 source, 1 relay	1 source, 1 relay	1 source 2 relay	1 source, 3 relay
Total power	2	2	3	4

Next, we will simulate and compare the AE-DF-MMSE system's performance with conventional systems' performance with the same number of receiving/transmitting antennas equal to 2, as shown in Figure 10. As a result, the BER of the AE-DF-MMSE system achieves a gain of 1.5 dB compared to the BER of the AE-AF-MMSE and DF-MMSE systems at BER = 10^{-3}. At the same time, the BER of AE-DF-MMSE is respectively better than the BER of AF-MMSE and DF-ZF [29] by 3 dB and 12 dB at the BER of 2.10^{-3}.

Figure 11 compares the BER performance of the AE-DF-MMSE system and the DF-MMSE system in cases where the system uses different numbers of antennas, N = 2, 3, 4, the threshold values of these systems, L_{BCE1}^{th} and L_{BCE2}^{th}, are equal to 10^{-3} and 10^{-6}, respectively. As the number of receiving/transmitting antennas increases, the performance of both DF-MMSE and AE-DF-MMSE systems improves because the systems receive spacial multiplexing gain. Specifically, at BER = 10^{-3}, the performance of the proposed systems achieves gains of 2 dB, 3 dB, and 4 dB, respectively, compared to the performance of the conventional systems with N = 2, 3, 4.

Figure 12 compares the BER of AE-DF-RTN and DF-MMSE systems equipped with two transmit-receive

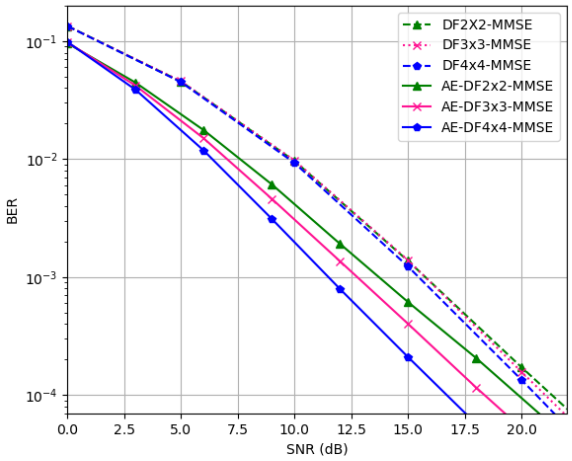

Figure 11. BER comparison between AE-DF-MMSE and conventional DF-MMSE with N = 2, 3, 4.

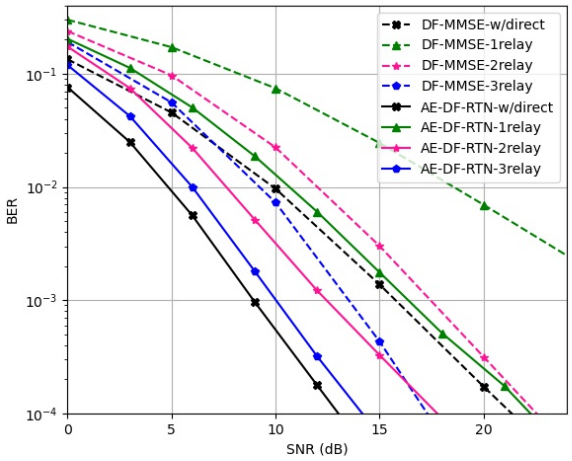

Figure 12. BER comparison between AE-DF-RTN and conventional DF-MMSE with and without direct paths.

antennas in cases with and without direct transmission paths. In the case where the system uses only one relay (*1relay*) and cooperates directly with the relay (*w/direct*), the AE-DF-RTN system achieves higher diversity gain than the DF-MMSE system, as the BER curve of the system using AE is steeper than that of the baseline system. Meanwhile, in the case of using two relays and three relays, the proposed system achieves increased utility without increasing diversity gain because all systems have the same BER curve slopes. When there is no direct transmission path, the system can use different numbers of relay paths, $L = 1, 2, 3$. Specifically, for $L = 2, 3$, $L_{BCE}^{th} = 5.10^{-6}$ the performance of the proposed system achieves gains of 3 dB and 5 dB, respectively, compared to the BER of the DF-MMSE system at BER = 10^{-3}. In addition, for $L = 1$, the BER of the proposed system is 11 dB better than the BER of DF-MMSE at BER = 8.10^{-3} and $L_{BCE}^{th} = 3.10^{-4}$. Additionally, The AE-DF-RTN system that uses one direct transmission path and one relay path (*w/direct*), trained with two sequential phases with $L_{BCE1}^{th} = 2.10^{-5}$, $L_{BCE2}^{th} = 5.10^{-7}$, achieves a better BER performance than the system using three relay paths (*3relay*). The system's performance is greatly enhanced when numerous relay paths are used. However, as shown in Table IV, the system must

pay a price in the form of higher computing complexity and power consumption.

5 Conclusion

The paper introduces AE-AF and AE-DF systems incorporating MMSE and RTN combinators, operating over a flat Rayleigh fading channel for on-body communication, in compliance with the IEEE 802.15.6 standard. Trained and synchronized learning parameters from the transmitter to the receiver, optimizing training parameters in a single phase or two sequential phases, the proposed schemes enhance the BER performance compared to conventional schemes such as AF-MMSE, DF-ZF, and DF-MMSE, assuming perfect CSI.

Additionally, the AE-DF systems demonstrate enhanced Bit Error Rate (BER) performance compared to the AE-AF systems, attributed to the absence of noise amplification at the relay node. However, the AE-DF systems incur increased computational complexity and a higher number of learning parameters at the relay node as trade-offs.

Moreover, the shadowing phenomenon is an important factor in shaping the characteristics of the body channel and significantly impacts the reliability of the communication process. Therefore, we continue to research solutions to reduce the computational complexity of the system and to address shadowing in WBANs.

References

[1] D. M. G. Preethichandra, L. Piyathilaka, U. Izhar, R. Samarasinghe, and L. C. De Silva, "Wireless Body Area Networks and Their Applications–A Review," *IEEE Access*, vol. 11, pp. 9202–9220, 2023.

[2] "IEEE Standard for Local and metropolitan area networks - part 15.6: Wireless Body Area Networks," *IEEE Std 802.15.6-2012*, pp. 1–271, 2012.

[3] S. L. Cotton, R. D'Errico, and C. Oestges, "A review of radio channel models for body centric communications," *Radio Science*, vol. 49, no. 6, pp. 371–388, 2014.

[4] F. Ullah, I. U. Islam, A. H. Abdullah, and A. Khan, *Future of Big Data and Deep Learning for Wireless Body Area Networks*. Springer Singapore, 01 2019, pp. 53–77.

[5] D. Quan, P. Thanh hiep, and R. Kohno, "Performance Analysis Method for IEEE 802.15.6 Based WBANs with Adaptive BCH Code Rates," *Wireless Personal Communications*, vol. 94, 06 2017.

[6] N. Dinh, P. Thanh hiep, O. Yua, and V. Son, "Controlling sequence length of DS-IR-UWB to enhance performance of multi-WBAN systems," *Journal of Electrical Engineering*, vol. 69, pp. 373–378, 09 2018.

[7] F. Hu, X. Liu, D. Sui, M. Shao, and L. Wang, "Performance analysis of reliability in wireless body area networks," *IET Communications*, vol. 11, no. 6, pp. 925–929, 2017.

[8] A. Arfaoui, A. Kribeche, and S. M. Senouci, "Cooperative MIMO for Adaptive Physical Layer Security in WBAN," in *Proceedings of the 2020 IEEE International Conference on Communications (ICC)*, 2020, pp. 1–7.

[9] Y. Zhang and B. Zhang, "A Relay-Aided Transmission Power Control Method in Wireless Body Area Networks," *IEEE Access*, vol. 5, pp. 8408–8418, 2017.

[10] Y. Peng and L. Peng, "A Cooperative Transmission Strategy for Body-Area Networks in Healthcare Systems," *IEEE Access*, vol. 4, pp. 9155–9162, 2016.

[11] T. O'Shea and J. Hoydis, "An Introduction to Deep Learning for the Physical Layer," *IEEE Transactions on Cognitive Communications and Networking*, vol. 3, no. 4, pp. 563–575, 2017.

[12] N. Chahat, G. Valerio, M. Zhadobov, and R. Sauleau, "On-Body Propagation at 60 GHz," *IEEE Transactions on Antennas and Propagation*, vol. 61, no. 4, pp. 1876–1888, 2013.

[13] M. Abbas, M. Ahmad, T. Hussain, and A. Mujahid, "Materials for Wearable Sensors," *Materials Innovations*, vol. 2, 07 2022.

[14] L. C. Tran, A. Mertins, X. Huang, and F. Safaei, "Comprehensive Performance Analysis of Fully Cooperative Communication in WBANs," *IEEE Access*, vol. 4, pp. 8737–8756, 2016.

[15] D. B. Smith and D. Miniutti, "Cooperative body-area-communications: First and second-order statistics with decode-and-forward," in *Proceedings of the 2012 IEEE Wireless Communications and Networking Conference (WCNC)*, 2012, pp. 689–693.

[16] Q. H. Abbasi, M. U. Rehman, K. Qaraqe, and A. Alomainy, *Advances in Body-Centric Wireless Communication Applications and state-of-the-art*. The Institution of Engineering and Technology, London, United Kingdom, 2016.

[17] C. He, Y. Liu, T. P. Ketterl, G. E. Arrobo, and R. D. Gitlin, "Performance evaluation for MIMO in vivo WBAN systems," in *Proceedings of the 2014 IEEE MTT-S International Microwave Workshop Series on RF and Wireless Technologies for Biomedical and Healthcare Applications*, 2014, pp. 1–3.

[18] Y. Wang and I. B. Bonev, "Characterization of the Indoor Multiantenna Body-to-Body Radio Channel," *IEEE Transactions on Antennas and Propagation*, vol. 57, no. 4, pp. 972–979, 2009.

[19] I. Khan and P. S. Hall, "Experimental Evaluation of MIMO Capacity and Correlation for Narrowband Body-Centric Wireless Channels," *IEEE Transactions on Antennas and Propagation*, vol. 58, no. 1, pp. 195–202, 2010.

[20] M. A. I. Oni and S. Dey, "On the Performance Analysis of Super Wide Band MIMO Antenna for Wireless Body Area Network (WBAN) Applications," in *Proceedings of the 2022 IEEE International Symposium on Antennas and Propagation and USNC-URSI Radio Science Meeting (AP-S/URSI)*, 2022, pp. 1896–1897.

[21] Q. Rubani, S. H. Gupta, and A. Rajawat, "A compact MIMO antenna for WBAN operating at Terahertz frequency," *Optik*, vol. 207, p. 164447, 2020.

[22] A. Rahim and N. C. Karmakar, "Virtual MIMO Using Energy Efficient Network Coding in Sleep Apnoea Monitoring Systems," in *4G Wireless Communication Networks*. River Publishers, 2022, pp. 375–399.

[23] Y. Yang, A. Rahim, and N. Karmakar, *5.8 GHz portable wireless monitoring system for sleep apnea diagnosis in wireless body sensor network (WBSN) using active RFID and MIMO technology*. Netherlands: Information Science Reference, 2013, pp. 264 – 303.

[24] W. Belaoura, K. Ghanem, M. A. Imran, A. Alomainy, and Q. H. Abbasi, "A Cooperative Massive MIMO System for Future In Vivo Nanonetworks," *IEEE Systems Journal*, vol. 15, no. 1, pp. 331–337, 2021.

[25] G. E. Arrobo and R. D. Gitlin, "Improving the reliability of wireless body area networks," in *Proceedings of the 2011 Annual International Conference of the IEEE Engineering in Medicine and Biology Society*, 2011, pp. 2192–2195.

[26] X. Li, G. Kang, X. Zhang, and D. Huang, "An energy-efficient cooperative MIMO strategy for Wireless Sensor Networks with intra-body channel," in *Proceedings of the 2012 International Symposium on Communications and Information Technologies (ISCIT)*, 2012, pp. 679–684.

[27] X. N. Tran, "Distributed Relay Selection for MIMO-SDM Cooperative Networks," *IEICE Transactions on Communications*, vol. E95B, pp. 1170–1179, 04 2012.

[28] H.-M. Kim, T.-K. Kim, M. Min, and G.-H. Im, "Low-Complexity Detection Scheme for Cooperative MIMO

Systems With Decode-and-Forward Relays," *IEEE Transactions on Communications*, vol. 63, no. 1, pp. 94–106, 2015.
[29] G. Choi, W. Zhang, and X. Ma, "Achieving Joint Diversity in Decode-and-Forward MIMO Relay Networks with Zero-Forcing Equalizers," *IEEE Transactions on Communications*, vol. 60, no. 6, pp. 1545–1554, 2012.
[30] K. Kedjar, M. E. Elazhari, L. Talbi, and M. Nedil, "Deep Learning Modeling of a WBAN-MIMO Channel in Underground Mine," *IEEE Access*, vol. 10, pp. 67 383–67 395, 2022.
[31] K. Liu, F. Ke, X. Huang, R. Yu, F. Lin, Y. Wu, and D. W. K. Ng, "DeepBAN: A Temporal Convolution-Based Communication Framework for Dynamic WBANs," *IEEE Transactions on Communications*, vol. 69, no. 10, pp. 6675–6690, 2021.
[32] A. Ali, K. Inoue, A. Shalaby, M. S. Sayed, and S. M. Ahmed, "Efficient Autoencoder-Based Human Body Communication Transceiver for WBAN," *IEEE Access*, vol. 7, pp. 117 196–117 205, 2019.
[33] X. Yuan, Z. Zhang, C. Feng, Y. Cui, S. Garg, G. Kaddoum, and K. Yu, "A DQN-Based Frame Aggregation and Task Offloading Approach for Edge-Enabled IoMT," *IEEE Transactions on Network Science and Engineering*, vol. 10, no. 3, pp. 1339–1351, 2023.
[34] L. Xiao, S. Hong, S. Xu, and H. Yang, "IRS-Aided Energy-Efficient Secure WBAN Transmission Based on Deep Reinforcement Learning," *IEEE Transactions on Communications*, vol. 70, no. 6, pp. 4162–4174, 2022.
[35] Y.-H. Xu, G. Yu, and Y.-T. Yong, "Deep Reinforcement Learning-Based Resource Scheduling Strategy for Reliability-Oriented Wireless Body Area Networks," *IEEE Sensors Letters*, vol. 5, no. 1, pp. 1–4, 2021.
[36] Y. Lu, P. Cheng, Z. Chen, Y. Li, W. H. Mow, and B. Vucetic, "Deep Autoencoder Learning for Relay-Assisted Cooperative Communication Systems," *IEEE Transactions on Communications*, vol. 68, no. 9, pp. 5471–5488, 2020.
[37] F. A. Aoudia and J. Hoydis, "Model-Free Training of End-to-End Communication Systems," *IEEE Journal on Selected Areas in Communications*, vol. 37, no. 11, pp. 2503–2516, 2019.
[38] A. Gupta and M. Sellathurai, "End-to-End Learning-Based Framework for Amplify-and-Forward Relay Networks," *IEEE Access*, vol. 9, pp. 81 660–81 677, 2021.
[39] T. Erpek, T. J. O'Shea, Y. E. Sagduyu, Y. Shi, and T. C. Clancy, *Deep Learning for Wireless Communications*. Development and Analysis of Deep Learning, Springer, 2020, pp. 223–266.
[40] T. J. O'Shea, T. Erpek, and T. C. Clancy, "Physical layer deep learning of encodings for the MIMO fading channel," in *Proceedings of the 55th Annual Allerton Conference on Communication, Control, and Computing (Allerton)*, 2017, pp. 76–80.
[41] J. Song, C. Häger, J. Schröder, T. J. O'Shea, E. Agrell, and H. Wymeersch, "Benchmarking and Interpreting End-toEnd Learning of MIMO and Multi-User Communication," *IEEE Transactions on Wireless Communications*, vol. 21, no. 9, pp. 7287–7298, 2022.
[42] T. T. T. Bui, X. N. Tran, and A. H. Phan, "Deep learning based MIMO systems using open-loop autoencoder," *AEU - International Journal of Electronics and Communications*, p. 154712, 2023.
[43] D. M. Barakah and M. Ammad-uddin, "A Survey of Challenges and Applications of Wireless Body Area Network (WBAN) and Role of a Virtual Doctor Server in Existing Architecture," in *Proceedings of the 2012 Third International Conference on Intelligent Systems Modelling and Simulation*, 2012, pp. 214–219.
[44] L. C. Tran, A. Mertins, X. Huang, and F. Safaei, "Comprehensive Performance Analysis of Fully Cooperative Communication in WBANs," *IEEE Access*, vol. 4, pp. 8737–8756, 2016.
[45] D. B. Smith, D. Miniutti, and L. W. Hanlen, "Characterization of the Body-Area Propagation Channel for Monitoring a Subject Sleeping," *IEEE Transactions on Antennas and Propagation*, vol. 59, no. 11, pp. 4388–4392, 2011.
[46] S. Cammerer, F. A. Aoudia, S. Dörner, M. Stark, J. Hoydis, and S. ten Brink, "Trainable Communication Systems: Concepts and Prototype," *IEEE Transactions on Communications*, vol. 68, pp. 5489–5503, 2019. [Online]. Available: https://api.semanticscholar.org/CorpusID:208513282
[47] R. Rosini and R. D'Errico, "Comparing On-Body dynamic channels for two antenna designs," in *Proceedings of the 2012 Loughborough Antennas and Propagation Conference (LAPC)*, 2012, pp. 1–4.
[48] S. L. Cotton and W. G. Scanlon, "Characterization and Modeling of the Indoor Radio Channel at 868 MHz for a Mobile Bodyworn Wireless Personal Area Network," *IEEE Antennas and Wireless Propagation Letters*, vol. 6, pp. 51–55, 2007.
[49] L. Liu, R. D'Errico, L. Ouvry, P. Doncker, and C. Oestges, "Dynamic Channel Modeling at 2.4 GHz for On-Body Area Networks," *J. Adv. Electron. Telecommun.*, vol. 2, 01 2011.
[50] D. B. Smith, D. Miniutti, T. A. Lamahewa, and L. W. Hanlen, "Propagation Models for Body-Area Networks: A Survey and New Outlook," *IEEE Antennas and Propagation Magazine*, vol. 55, no. 5, pp. 97–117, 2013.
[51] D. Kingma and J. Ba, "Adam: A Method for Stochastic Optimization," *International Conference on Learning Representations*, 12 2014.

Thi Thanh Tam Bui is currently working toward the PhD. degree at the Electronic Institute at Academy of Military Science and Technology. She obtained her bachelor degree in radio-electronics from Le Quy Don Technical University, Vietnam in 2009. She received her master of engineering (ME) in electronic engineering from Le Quy Don Technical University in 2016. Her research interests are in the area of signal processing, biomedical engineering MIMO systems and deep learning.

Xuan Nam Tran is currently a professor at the Department of Communications Engineering at Le Quy Don Technical University Vietnam. He received his master of engineering (ME) in telecommunications engineering from the University of Technology Sydney, Australia in 1998, and doctor of engineering in electronic engineering from The University of Electro-Communications, Japan in 2003. From November 2003 to March 2006 he was a research associate at the Information and Communication Systems Group, Department of Information and Communication Engineering, The University of Electro-ommunications, Tokyo, Japan. Dr. Tran's research interests are in the areas of adaptive antennas, spacetime processing, space-time coding and MIMO systems. Dr. Tran is a recipient of the 2003 IEEE AP-S Japan Chapter Young Engineer Award. He is a member of IEEE, IEICE, and the Radio-Electronics Association of Vietnam.

Anh Huy Phan received the Bachelor's degree in physics from Hanoi University of Science, Hanoi, Vietnam, in 2003, received the M.Eng. degree in telecommunications from the University of Melbourne, Melbourne, Australia, in 2007, and received the Ph.D. degree in Electrical from the School of Electrical Engineering and Telecommunications, University of New South Wales, Sydney, Australia, in 2014. Now, he is a reseacher at Academy of Military Science and Technology, Ha Noi, Viet Nam. His research interests are in signal processing for communications, currently on optimization problems in cognitive radio, wireless relay networks, MIMO detection and visual localization for UAVs.